Applied Biological Research 28(1): 21-31; (2026)
DOI: 10.48165/abr.2026.28.3

NANOENCAPSULATION OF LEMONGRASS OIL AS A NOVEL STRATEGY TO COMBAT ANTIMICROBIAL RESISTANCE

V. Chetana, S. Suja Rani*, A.R. Nisha, Suresh N. Nair and Divya Sebastian

Department of Veterinary Pharmacology and Toxicology, College of Veterinary and Animal Sciences, Kerala Veterinary and Animal Sciences University, Mannuthy, Thrissur - 680 651, Kerala (India)
*****e-mail: *sujarani@kvasu.ac.in*

(Received 17 May, 2025; accepted 29 December, 2025)

ABSTRACT

The increasing prevalence of multidrug-resistant (MDR) bacteria has necessitated to formulate alternative antimicrobial strategies. This study evaluated the antibacterial efficacy of lemongrass oil (LGO) nanoencapsulated in chitosan nanoparticles against MDR *Staphylococcus aureus* (MDRSA) and *Escherichia coli* (MDREC). Ionic gelation technique was used to synthesise lemongrass oil loaded chitosan nanoparticles which were further characterized by dynamic light scattering (DLS), field emission scanning electron microscopy (FESEM), UV-Visible spectrophotometry, and FTIR analysis. A significant increase in particle size from 168.7 nm for plain chitosan nanoparticles to 318.7 nm following LGO encapsulation, with acceptable polydispersity was observed through DLS, while FESEM confirmed spherical nanoparticles with smooth surfaces and sizes ranging from 50 to 150 nm. Encapsulation efficiency and loading capacity range was 41.7-91.17 and 21.36-74.36%, respectively, with maximum values observed at a 1:1 chitosan-to-LGO ratio. Nanoencapsulation significantly enhanced the antibacterial activity, with LGO-loaded nanoparticles exhibiting lower MIC values as compared to the free LGO against MDRSA (0.052% vs 0.125%) and MDREC (0.0104% vs 0.25%). Similarly, reduced MBC values were observed for the nanoformulation. These findings demonstrate that chitosan-based nanoencapsulation significantly improves the antibacterial efficacy of lemongrass oil against MDR pathogens.

Keywords: Antibacterial activity, characterization, lemongrass oil, multidrug resistant, nanoencapsulation

INTRODUCTION

The escalating threat of antimicrobial resistance (AMR) is a major challenge to the global healthcare due to the emergence of multidrug-resistant (MDR) microbes. Recognized as one of the serious public health threats, AMR as per conservative estimates could cause up to 10 million deaths annually by 2050 in absence of effective interventions (WHO, 2014; O'Neill, 2016). Of particular concern are the ESKAPEE pathogens, including *Staphylococcus aureus* and *Escherichia coli*, which show a marked ability to develop resistance to multiple antimicrobial classes (Mulani *et al.,* 2019; Thomas e*t al.,* 2019). Further, the decreasing efficacy of conventional antibiotics has aroused the interest in alternative antimicrobial agents. Essential oils (EOs) have gained attention due to their broad-spectrum antimicrobial activity and their ability to act through multiple mechanisms, thereby reducing the likelihood of resistance development (Raut *et al.,* 2014; Veras and Karuppayil, 2014). These bioactive plant-derived compounds, rich in terpenoids and phenylpropanoids, exert antimicrobial effects primarily through disruption of bacterial cell membranes and interference with essential cellular processes (Holley and Patel, 2005; Bakkali *et al.,* 2008).

Lemongrass oil (LGO), obtained from *Cymbopogon* species, has widely been reported to possess antibacterial activity against both Gram-positive and Gram-negative bacteria, including *S. aureus* and *E. coli* (Onawunmi and Ogunlana, 1986; Cimanga *et al.*, 2002). Despite this potential, the use of essential oils is limited due to their high volatility, chemical instability, poor aqueous solubility, and susceptibility to environmental degradation (Schweiggert *et al.*, 2007).

Nanoencapsulation has emerged as an effective strategy to overcome these limitations by improving the stability, bioavailability, and controlled release of essential oils. In this context, chitosan-based nanoparticles have received considerable attention owing to their biocompatibility, biodegradability, and inherent antimicrobial properties. Recent studies have demonstrated enhanced antibacterial efficacy of essential oils when nanoencapsulated in chitosan matrices, particularly against resistant bacterial strains (Donsí *et al.*, 2011; Hosseini *et al.*, 2013). Therefore, the present study was aimed to evaluate the antibacterial efficacy of lemongrass oil nanoencapsulated in chitosan nanoparticles against multidrug-resistant *Staphylococcus aureus* and *Escherichia coli*. The study also characterized the physicochemical properties of nano-formulation and compared its antibacterial activity with that of unencapsulated lemongrass oil using *in vitro* assays.

MATERIALS AND METHODS

Chemicals and test strains

Chitosan (MMW), sodium tripolyphosphate (S-TPP), glacial acetic acid, dichloromethane (DCM), mannitol salt agar (60062), Mueller Hinton agar (24756), and resazurin sodium extrapure AR dye (42650) were procured from Sisco Research Laboratories, India. Tween 20 (SE7S67310) was purchased from Merck Life Science, Mumbai, while tween 80 (GRM159-100G), cationated Mueller Hinton broth (M1657), nutrient broth (M002), brain heart infusion agar (M210), brain heart infusion broth (M210), and crystal violet (S012) were purchased from Himedia, India. Lemongrass oil was procured from Synthite Industries Pvt. Ltd., Kerala. The antibiotic discs including ampicillin (10 µg), gentamicin (10 µg), chloramphenicol (30 µg), amoxycilllin-clavulinic acid (20/10 µg), tetracycline (30 µg), cotrimoxazole **(**25 µg) and Hexa G-plus 13 (HX040) containing tetracycline (TE, 30 µg), gentamicin (GEN, 10 µg), chloramphenicol (C, 30 µg), cefotaxime (CTX, 30 µg), cloxacillin (COX, 5 µg), and co-trimoxazole (COT, 25 µg) were purchased from Himedia, India. Five isolates, each of *Staphylococcus aureus* and *Escherichia coli,* isolated from clinical mastitis samples, were procured from the Department of Veterinary Microbiology, College of Veterinary and Animal Sciences, Kerala Veterinary and Animal Sciences University (India).

Gas chromatography-mass spectroscopic analysis of lemongrass oil

The GC-MS analysis was conducted using Shimadzu GC-MS Model No.: QP2010S (GCMS Solutions) equipped with Rxi-5Sil MS capillary column (30 m x 0.25 mm, 0.25 µm thickness) for the analysis of chemical composition of LGO. The column temperature was initially held at 80°C for 4 min and then increased to 280°C @ 5°C min^{-1} and held at 280°C for 6 min. The injector and interface temperature were 200 and 280°C, respectively. The ion source temperature was 200°C. For GC-MS detection, an electron ionization system with ionization energy 70 eV was used over a scan range of 50- 500 m/z. Carrier gas helium was used @ 1.00 mL min^{-1} in split 1:50 with injection volume of 1 µL. The chemical constituents of LGO were identified by comparing the obtained mass spectra with those available in NIST 11 and Wiley 8 mass spectral libraries based on spectral similarity.

Synthesis of LGO encapsulated chitosan nanoparticles

The LGO-loaded chitosan nanoparticles (LGOCSNPs) were synthesized following the method of Das *et al*. (2019). Initially, a 1.5% chitosan solution was prepared using 1% glacial acetic acid. Tween 80 was added to this chitosan solution, and thoroughly mixed for 2 h at 45°C to form a homogeneous

mixture. Various amounts of LGO (0.00, 0.06, 0.12, 0.18, 0.24, and 0.30 g) were used to achieve different chitosan to LGO weight ratios: 1:0, 1:0.2, 1:0.4, 1:0.6, 1:0.8, and 1:1. Lemongrass oil was dissolved in 4 mL DCM and introduced to the chitosan solution during homogenization at 13000 rpm for 10 min at 4°C. Then 0.4% S-TPP solution was added dropwise while stirring magnetically, and the mixture was allowed to react for 40 min. The emulsion was centrifuged at 10000 rpm for 30 min at 4°C to collect the nanoparticles, which were washed 2-3 times with distilled water. The resulting pellet was re-suspended in double distilled water and subjected to sonication for 4 min (1-sec pulse on, 1-sec pulse off) in an ice bath. The emulsion was freeze-dried using a lyophilizer at -52°C for 72 h for subsequent physicochemical characterization.

Characterization of nanoencapsulated LGO

Dynamic light scattering (DLS): DLS analysis was performed following standard procedures (Bagheri *et al*., 2020), with slight modifications. Samples were prepared by mixing 10-20 µL colloidal dispersion with 3 mL distilled water until a clear to slightly hazy sample solution was obtained. Then 3 mL diluted solution was transferred to a quartz cuvette for DLS analysis to determine the particle size through repeated trial and error iterations.

Field emission scanning electron microscopy (FESEM): The morphology of chitosan nanoparticles and LGO loaded chitosan nanoparticles was studied using FESEM (Carl Zeiss, Germany). The nanoparticle solution (10 µL) was drop-cast onto a stub, followed by drying. Then dried film was coated with gold, using an ion sputter and examined at an accelerating voltage of 20 kV (Deepika *et al*., 2021).

Attenuated total reflectance - Fourier transform infrared spectroscopy (ATR-FTIR): Interaction of different components in nanoparticle formulation was assessed by FTIR spectra of pure chitosan powder, LGO, chitosan nanoparticle and encapsulated LGO nanoparticle (Deepika *et al*., 2021). The spectra were obtained using a Perkin Elmer Spectrum-2 FTIR spectrometer with sampling station equipped with ATR accessory (Perkin Elmer, UK). The samples were scanned at room temperature, in the range 400-4,000 cm^{-1} at a speed of 2 mm sec^{-1} and a resolution of 4 cm^{-1}. The FTIR analysis was performed to evaluate the possible interactions between chitosan and LGO by comparing the characteristic peaks of the individual components and the formulated nanoparticles.

Determination of encapsulation efficiency and loading capacity of nanoencapsulated LGO

The loaded LGO in CSNPs was determined by UV-visible spectrophotometry (Perkin Elmer) by indirect method i.e., by estimating the amount of unencapsulated drug present in the supernatant obtained after centrifugation during synthesis (Deepika *et al.*, 2021). Absorbance maxima of citral dissolved in ethanol was 273.5 nm ($y = 0.0193x + 0.0784$, $R^2 = 0.9956$). The 30 µL LGOCSNPs of different concentrations (chitosan to LGO weight ratio: 1:0, 1:0.2, 1:0.4, 1:0.6, 1:0.8 and 1:1.) were added to 3 mL ethanol and mixed properly for 5 min. The amount of LGO loaded in CSNPs was determined by measuring its optical density and comparing it with standard curve of citral constructed at 273.5 nm. The per cent encapsulation efficiency and loading capacity of LGO were calculated using the formula:

$$Encapsulation\ efficiency\ (\%) = \frac{Total\ amount\ of\ LGO\ added - Amount\ of\ LGO\ loaded}{Total\ amount\ of\ LGO\ added} \times 100$$

$$Loading\ capacity\ (\%) = \frac{Total\ amount\ of\ LGO\ loaded}{Weight\ of\ LGOCSNPs} \times 100$$

Antibiotic sensitivity testing by Kirby-Bauer disc diffusion method

In this study, the Kirby-Bauer disk diffusion method (Bauer *et al*., 1996) was employed to evaluate the antibiotic susceptibility of MDRSA and MDREC isolates. Briefly, bacterial colonies were suspended in sterile saline to match the turbidity of a 0.5 McFarland standard. The bacterial suspension was then evenly spread over Mueller-Hilton agar plates using a sterile cotton swab. The antibiotic discs Hexa G-plus 13 containing tetracycline (TE, 30 µg), gentamicin (GEN, 10 µg),

chloramphenicol (C, 30 µg), cefotaxime (CTX, 30 µg), cloxacillin (COX, 5 µg), co-trimoxazole (COT, 25 µg) for *S. aureus* and ampicillin (AMP, 10 µg), amoxicillin-clavulanate (AMC, 20/10 µg), chloramphenicol (C, 30 µg), tetracycline (TE, 30 µg), cotrimoxazole (COT, 25 µg), gentamicin (GEN, 10 µg) for *E. coli* were placed on the agar surface, and plates incubated at 37ºC for 18 h. The diameters of inhibition zones were measured and interpreted as per the CLSI guidelines (CLSI, 2023).

Antimicrobial susceptibility of MDR S. aureus and E. coli against LGO

The Kirby-Bauer disk diffusion assay (Bauer *et al*., 1996) for lemongrass oil (LGO) was performed using Mueller-Hinton agar (MHA). Sterile 6 mm diameter discs were impregnated with 10 µl of various LGO dilutions in 5% tween 20 (1:1, 1:2, 1:5, and 1:10 ratios) and placed symmetrically on the agar surface using sterile forceps. A disc moistened with 5% tween 20 served as a vehicle control. The plates were sealed with sterile parafilm to prevent evaporation and incubated at 35°C for 24 h. Zones of inhibition >10 mm were considered significantly inhibitory as per Fu *et al*. (2007).

Micro-broth dilution method for minimum inhibition concentration (MIC) assay

A modified resazurin microtiter plate assay (Balouri *et al.*, 2016) was used to determine the MIC. In a 96 wells flat bottom microtiter plate, 100 µL test cultures (@ 5×10^5 CFU mL^{-1}) were separately co-incubated with decreasing concentrations of LGO and in 100 µL cation adjusted Muller-Hinton broth. Pilot studies were conducted initially to determine the concentrations. Broth control (medium only), growth control (medium with bacterial inoculum), and vehicle control (medium with bacterial inoculum and 0.5% tween 20 without test compounds) were included in all assays. After incubation at 37ºC for 24 h, 30 µL resazurin dye (0.01%) was added to all the wells to determine the dye reduction (from purple to pink) and thereby the bacterial inhibition. The lowest concentrations of LGO and LGOCSNPs without visible growth were designated as MIC (Sanchez *et al*., 2016). The experiment was repeated thrice.

Determination of minimum bactericidal concentration (MBC)

The MBC was determined by employing the method of Misra and Sahoo (2012). The bacterial suspension in 96 well microtitre plate with more or equal to MIC, were used for MBC determination. The suspension was streaked onto sterile nutrient agar plates (NA) and observed for bacterial growth after incubation at 35ºC for 24 h. The lowest concentration of test substance which visibly inhibited bacterial growth on NA was defined as MBC. Each test was done in triplicates against 6 MDR isolates.

Statistical analysis

Experiments were conducted in a completely randomized design using six groups: one control group consisting of chitosan nanoparticles without LGO (CSNPs) and five treatment groups with different concentrations of LGO-loaded chitosan nanoparticles. Each group was tested in triplicate (n = 3). All the results were expressed as mean ± SE with 'n' as number of replicates. Statistical analysis was performed using SPSS software version 21. The data were analysed by one-way analysis of variance (ANOVA) followed by Duncan's multiple comparison test. Statistical significance was set at $p < 0.05$.

RESULTS AND DISCUSSION

Gas chromatography-mass spectroscopic analysis for composition of lemongrass oil

In this study, 27 distinct compounds were identified in *Cymbopogon flexuosus* oil by using GC-MS analysis (Table 1). Terpenoids, especially geranial (37.61%), neral (32.82%), geraniol (8.98%), and geranyl acetate (4.37%), were the predominant ingredients. Caryophyllene (2.15%), γ-cadinene (2.15%), isocitral (1.49%), β-linalool (1.3%), camphene (1.21%), and 4-nonanone (1.15%) were some other significant ingredients. One important component of lemongrass oil, citral, made up 70.43% of the overall oil. These results are in line with Jisha *et al*. (2020), who found that 44% of total oil content in *C. flexuosus* was composed of citral, which made up 71.81%.

Table 1: Chemical composition of lemongrass oil (LGO) analyzed by GC-MS

S. No.	Name of the compound	Class of compound	Molecular formula	Molecular weight (g mole^{-1})	Retention time (min)	Height	Peak area (%)
1	Geranial	Monoterpenoid	$C_{10}H_{16}O$	152.23	20.010	24.44	37.61
2	Neral	Monoterpenoid	$C_{10}H_{16}O$	152.23	18.625	25.53	32.82
3	Geraniol	Monoterpenoid	$C_{10}H_{10}O$	154.25	19.177	8.51	8.98
4	Geranyl acetate	Monoterpenoid	$C_{12}H_{20}O_2$	196.29	24.639	7.87	4.37
5	Caryophyllene	Bicyclic sesquiterpene	$C_{15}H_{24}$	204.35	26.288	3.58	2.15
6	γ-Cadinene	Bicyclic sesquiterpene	$C_{15}H_{24}$	204.35	30.140	3.11	2.15
7	Isocitral	Monoterpenoid	$C_{10}H_{16}O$	152.23	15.870	3.09	1.49
8	β-Linalool	Monoterpenoid	$C_{10}H_{18}O$	154.25	12.383	3.13	1.30
9	Camphene	Monoterpenoid	$C_{10}H_{16}$	136.23	6.743	3.57	1.21
10	4-Nonanone	Aliphatic ketone	$C_9H_{18}O$	142.24	11.170	2.79	1.15

The predominance of citral likely contributes to the well-established antibacterial and anti-biofilm properties of LGO, as this compound can disrupt lipid bilayer interactions and inhibit microbial growth (Kotzekidou *et al*., 2008). Minor constituents such as geraniol and caryophyllene may contribute synergistically to enhance the overall bioactivity (Mukarram *et al*., 2021).

Dynamic light scattering (DLS)

DLS analysis revealed that chitosan nanoparticles (CSNPs) had an average diameter of 168.7 nm, which increased significantly to 318.7 nm upon incorporation of lemongrass oil (LGO) [Fig. 1]. This alteration aligns with findings of Keawchaoon and Yoksan (2011) and Hosseini *et al*. (2013), who reported similar increase on successful encapsulation of essential oils. Hosseini *et al*. (2013) noted that plain chitosan NPs measured 281.5 nm, while those loaded with oregano-essential oil ranged from 309.8 to 402.2 nm. The polydispersity index (PDI) indicated a monodisperse distribution for CSNPs at 0.038 as compared to 0.302 for LGO-loaded chitosan nanoparticles (LGO-CSNPs), suggesting a wider size distribution. These findings reflect the impact of encapsulated substances on the physical characteristics of chitosan-based nano-carriers and are consistent with Hadidi *et al*. (2020), who reported PDI values between 0.117 and 0.337.

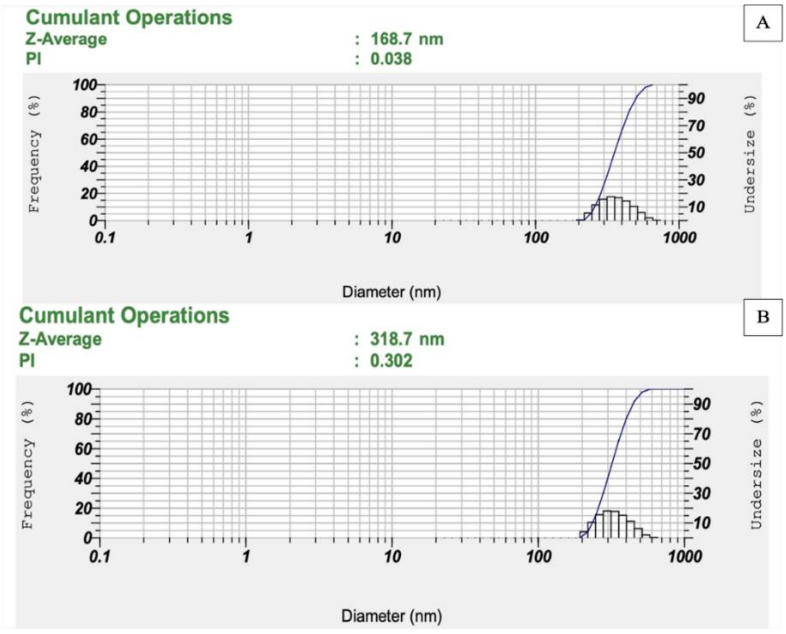

Fig. 1: Particle size and PDI of nanoparticles characterized by DLS in CSNPs (A) and LGOCSNPs (B)

Field emission scanning electron microscopy

FESEM was used to assess the morphology and dimensions of chitosan nanoparticles (CSNPs) and LGO-loaded chitosan nanoparticles (LGOCSNPs). Both types were found to be spherical with smooth surfaces (Fig. 2), attributed to effective ionic interactions between chitosan and sodium tripolyphosphate. CSNPs measured between 56.88 and 82.47 nm, while LGOCSNPs ranged from 70.56 to 159.32 nm, indicating successful encapsulation of LGO within the chitosan matrix. This increase

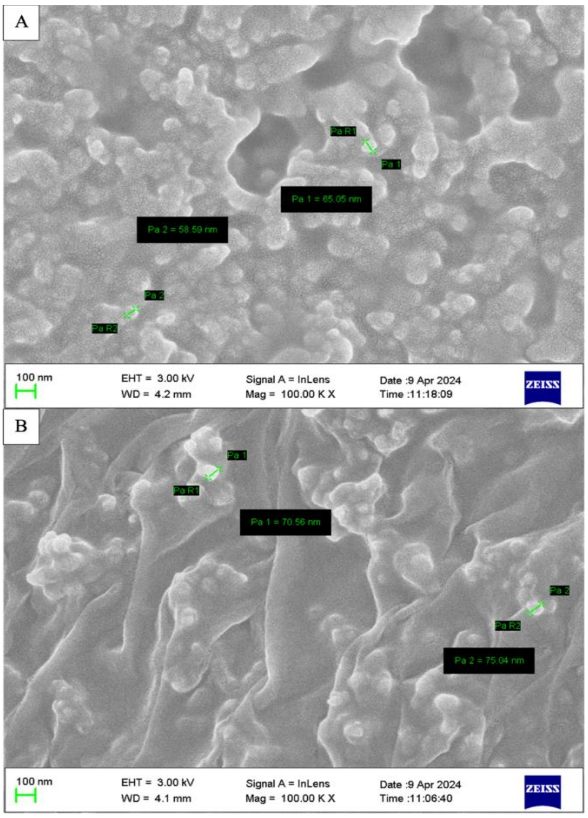

Fig. 2: Field emission scanning electron microscopic image of CSNPs (A) & LGOCSNPs (B)

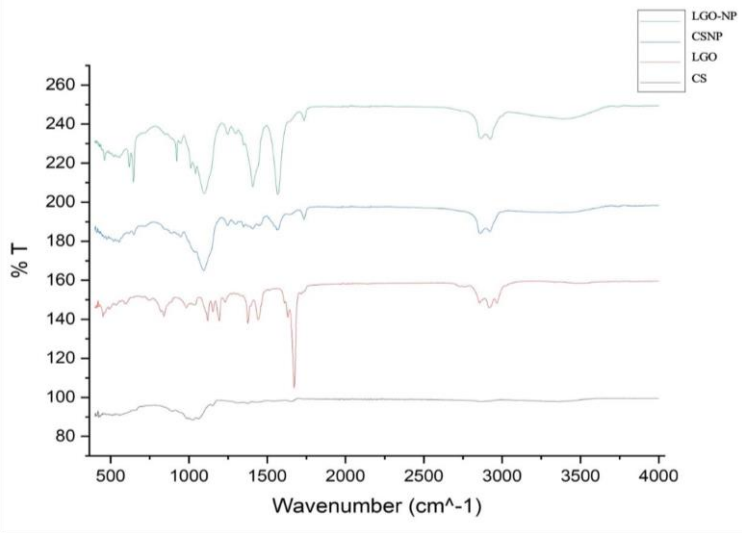

Fig. 3: Comparison of Fourier transform infrared spectra of chitosan powder, pure LGO, CSNPs and LGOCSNPs

in size is consistent with Lertsutthiwong *et al.* (2008) and Sotelo-Boyás *et al.* (2017) who reported almost similar findings with essential oils in alginate and chitosan nanocapsules. All nano-particles remained under 500 nm in diameter, thus corroborate with the DLS size measurements.

Attenuated total reflectance - Fourier transform infrared spectroscopy (ATR-FTIR)

The FTIR analysis of chitosan and its nanoparticles revealed several significant wavenumbers. For pure chitosan, key peaks included O-H stretching at 3380-3400 cm^{-1}, amide I at 1659 cm^{-1}, amide II at 1565 cm^{-1}, amide III at 1371 cm^{-1}, and pyranoside ring vibrations at 649 cm^{-1} (Fig. 3). In chitosan nano-particles (CSNPs), the absence of amide I peak and the emergence of a new peak at 1735.31 cm^{-1} showed successful crosslinking with sodium tripolyphosphate (STPP). The lemongrass oil spectrum displayed peaks for C-H stretching at 2966-2856 cm^{-1}, C=O stretching at 1672-1632 cm^{-1}, CH_2 and CH_3 bending at 1442-1377 cm^{-1}, and C-O stretching at 1193-1120 cm^{-1} (Fig. 3). In LGOCSNPs, a new peak at 3392.95 cm^{-1} suggested a possible hydrogen bonding, while the retention of C-H and C-O stretching peaks confirmed the successful incorporation of LGO into the nanoparticles (Deepika *et al.*, 2021). These observations highlight the structural changes and interactions that occur during encapsulation process. The standard curve generated for citral demonstrated a high linearity, with an R^2 value of 0.9956. The encapsulation efficiency and loading capacity values varied from 41.7 to 91.17% and 21.36 to 74.36%, respectively, which revealed that the encapsulation process enhanced the stability.

Determination of encapsulation efficiency and loading capacity of nanoencapsulated LGO

Citral, the predominant component of lemongrass oil (LGO), exhibited a maximum absorption at 273.5 nm in ethanol when analyzed within a range of 200-400 nm by using UV-vis spectrophotometry (Ghazali *et al.*, 2021). The standard curve generated for citral demonstrated a high linearity, with a correlation between both encapsulation efficiency and loading capacity and the initial concentration of

LGO, with maximum values observed at a 1:1 weight/volume ratio of chitosan to LGO (Table 2). This trend aligns with the findings of Benavides *et al*. (2016) and Shetta *et al*. (2019), who also reported optimal loading capacities at elevated concentrations of essential oil and polymer during the preparation of alginate microspheres and chitosan nano-particles, respectively, using the ionic-gelation method. This trend can be attributed to the greater availability of LGO molecules for incorporation within the chitosan matrix, allowing more efficient encapsulation as the oil concentration rise.

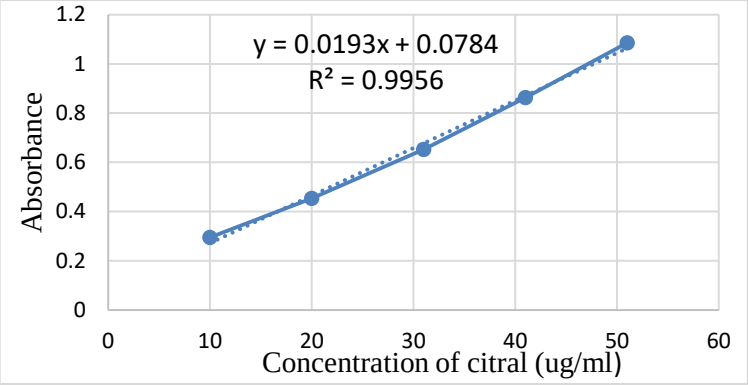

Fig. 4: Standard curve of citral in ethanol at 273.5 nm

Antibiotic sensitivity testing by Kirby-Bauer disc diffusion method

In this study, antibiotic susceptibility tests were conducted on five isolates each of *S. aureus* and *E. coli* using different antibiotic discs. All the isolated exhibited resistance to three or more than three different classes of antibiotics with MAR index ranging from 0.5 to 0.83, indicating a very high resistance (Osundiya *et al*., 2013). Such elevated MAR values suggest exposure to environments with frequent antibiotic use and highlight the need for alternative antimicrobial strategies, such as essential oil-loaded nanoparticles.

Table 2: Encapsulation efficiency and loading capacity of different ratios of CS: LGO

CS: LGO	OD of supernatant	Encapsulation efficiency (%)	Loading capacity (%)
1:0.2	0.304^{a} ± 0.0024	41.68^{e} ± 0.628	21.36
1:0.4	0.287^{b} ± 0.0008	73.04^{d}± 0.098	57.18
1:0.6	0.286^{bc} ± 0.0005	82.10^{c} ± 0.045	62.93
1:0.8	0.282^{c} ± 0.0011	86.81^{b} ± 0.074	68.42
1:1.0	0.249^{d} ± 0.000	91.16^{a} ± 0.002	74.36

Antimicrobial susceptibility of MDR S. aureus and E. coli against LGO

In this study, disc diffusion method was applied to assess the efficacy of LGO at various dilutions (1:1, 1:2, 1:5, and 1:10 in 0.5% tween 20) against MDRSA and MDREC isolates. The findings revealed that LGO exhibited significant antimicrobial activity against both MDRSA and MDREC (Fig. 5), with inhibition zones exceeding 10 mm in all dilutions, except 1:10 for MDRSA and at 1:5 and 1:10 dilutions for MDREC (Table 3). The inhibition zones increased with higher LGO concentrations, likely due to the greater availability of bioactive compounds to interact with bacterial cell membranes, whereas lower concentrations were insufficient to cause measurable effects. No inhibition was observed in vehicle-only controls, and a reduction in the inhibition zone size was noted with increasing dilution (Table 3). These results are in line with Naik *et al*. (2010) and (Sanchez *et al*., 2016) where Gram-positive bacteria such as *S. aureus* and *B. subtilis* demonstrated greater sensitivity to lemongrass oil compared to Gram- negative *E. coli*, possibly because Gram-negative bacteria possess an outer membrane that limits essential oil penetration.

Table 3: Zone of inhibition of different dilution of LGO against MDR *S. aureus* (MDRSA) and MDR *E. coli* (MDREC)

Concentration ratio	Mean ± SE of ZOI (mm)	
	MDRSA	MDREC
1: 1	26.00^{a} ± 0.35	19.60^{a} ± 0.43
1: 2	20.79^{b} ± 0.41	13.80^{b} ± 0.37
1: 5	11.00^{c} ± 0.35	9.90^{c} ± 0.60
1: 10	7.30^{d} ± 0.30	5.40^{d} ± 0.24

Significant at 0.01 level

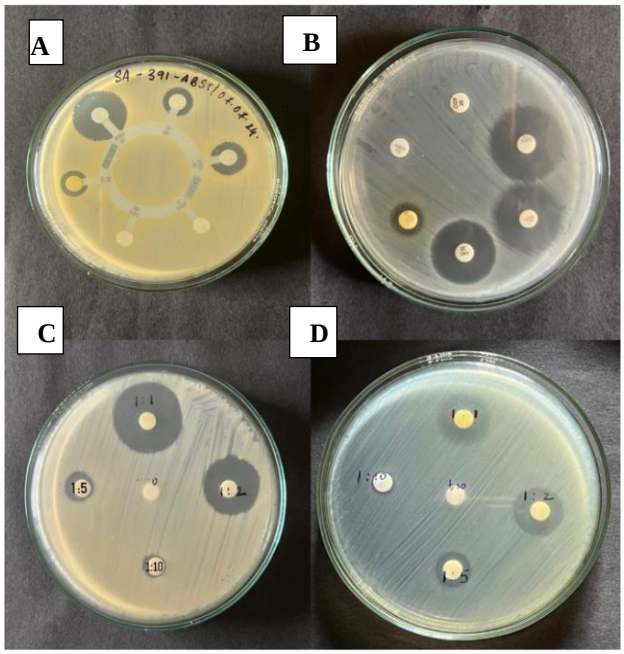

Fig. 5: A) Antimicrobial susceptibility test of *S. aureus* isolate using Hexa G-plus 13 discs (CTX - Cefotaxime, COX - Cloxacillin, C - Chloramphenicol, TE - Tetracycline, COT - Cotrimoxazole, GEN - Gentamicin) B) Antimicrobial susceptibility test of *E. coli* isolate using individual antibiotic discs (AMP - Ampicillin, AMC - Amoxicillin-clavulanate, C - Chloramphenicol, TE - Tetracycline, COT - Cotrimoxazole, GEN - Gentamicin); C) Zones of inhibition of LGO at dilutions 1:1, 1:2, 1:5 and 1: 10 against MDR-SA isolates; D) Zones of inhibition of LGO at dilutions 1:1, 1:2, 1:5 and 1: 10 against MDR-EC isolates; LGO: Lemongrass oil; MDR-SA: Multidrug resistant *Staphylococcus aureus*; MDR-EC: Multidrug resistant *Escherichia coli*.

Minimum inhibitory concentration (MIC)

The MIC, defined as the minimum concentration of an antibacterial agent that entirely inhibits visible growth under controlled *in vitro* conditions, was determined by micro-broth dilution method (EUCAST, 2020). The LGO showed an MIC of 0.125% against MDRSA isolates, while LGOCSNPs demonstrated a notably lower MIC of 0.052% (Fig. 6). For MDREC isolates, the MIC of LGO was 0.25%, whereas LGOCSNPs achieved an MIC of 0.0104%. These findings are consistent with Hasani and Hasani (2018), who reported that nanoencapsulated thyme oil had superior antibacterial activity against *S. aureus* and *E. coli* as compared to its unencapsulated counterpart. Hassanshahian *et al*. (2020) have reported that the essential oils encapsulated in chitosan nanoparticles exhibited lower MIC values as compared to their free forms. Also, the nanoemulsions were more effective in inhibiting the growth of various pathogenic bacteria such as *S. aureus and E. coli* at concentrations lower than those required for the unencapsulated essential oil.

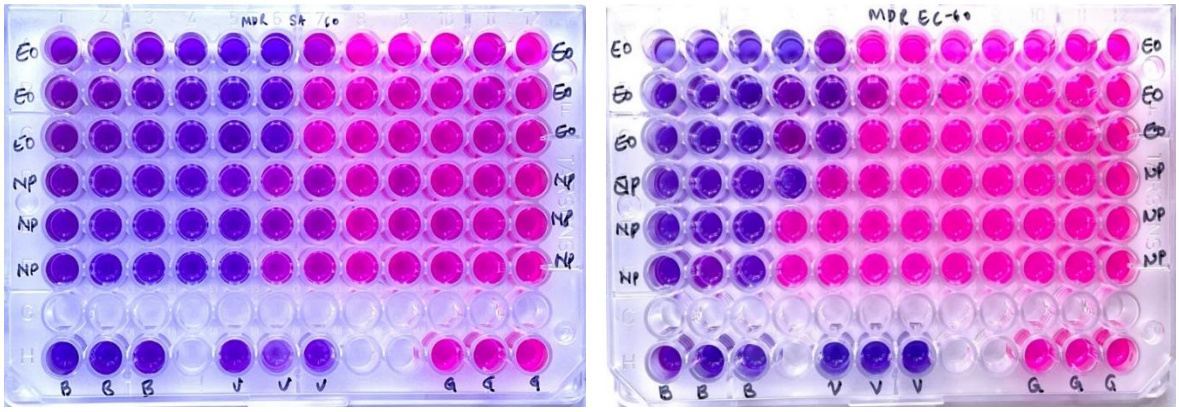

(A) **(B)**

Fig. 6: MIC of LGO and LGOCSNPS against MDR-SA (A) and MDR-EC (B) using micro-broth dilution technique; EO - LGO; NP - LGOCSNPS, B - Broth control; V - Vehicle control; G - Growth control

Determination of minimum bactericidal concentration (MBC)

The minimum bactericidal concentration represents the lowest concentration of an antimicrobial

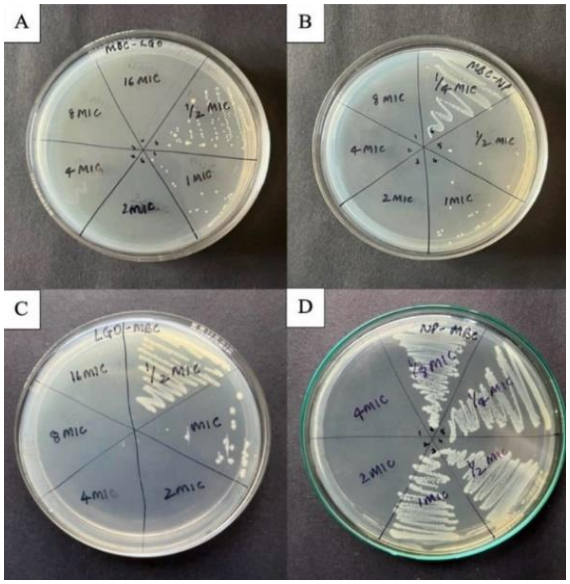

Fig. 7: MBC of (A) LGO and (B) LGOCSNPs against MDRSA isolates; MBC of (C) LGO and (D) LGOCSNPs against MDREC isolates

agent required to kill a bacterial organism, determined by sub-culturing broth dilutions that inhibit growth, streaking them onto agar, and incubating for 24-48 h. The MBC is identified as the lowest concentration that prevents bacterial growth on the agar, indicating that only nonviable cells remain (Sykes and Rankin, 2014). In this study, both LGO and LGOCSNPs exhibited MBC values double that of their respective MICs against *S. aureus* and *E. coli* (Fig. 7). However, LGOCSNPs demonstrated significantly lower MBCs as compared to LGO, highlighting their superior bactericidal efficacy. These findings align with Hassanshahian *et al.* (2020), who also reported that chitosan nanoparticle-encapsulated essential oils have lower MIC and MBC values as compared to their unencapsulated counterparts, with nano-emulsions requiring lower concentrations to inhibit pathogenic bacteria.

Conclusion: This study demonstrated that nanoencapsulation of lemongrass oil (LGO) in chitosan nanoparticles significantly enhances its antibacterial efficacy against multidrug-resistant *Staphylococcus aureus* and *Escherichia coli*. The LGO-loaded chitosan nanoparticles showed significantly lower MIC and MBC values compared to free LGO, highlighting the potential of this nanoformulation as a promising alternative in the fight against antimicrobial resistance. These findings pave the way for further research into the development of nanoencapsulated essential oils as effective natural antimicrobial agents.

Acknowledgements: The author is grateful to the Kerala Veterinary and Animal Sciences University, Mannuthy (India) for providing M.V.Sc. research grant and logistic facilities for this study.

Ethical statement: In present study there is no use of animals or humans so no ethical approval was required.

Conflict of interest: The authors declare that they have no conflict of interest.

REFERENCES

Bakkali, F., Averbeck, S., Averbeck, D. and Idaomar, M. 2008. Biological effects of essential oils - A review. *Food and Chemical Toxicology*, **46**(2): 446-475.

Bauer, A.W., Kirby, W.M., Sherris, J.C. and Truck, N. 1996. Antimicrobial susceptibility testing by a standardized single disk method. *American Journal of Clinical Pathol*ogy, **45**: 493-496.

Benavides, S., Cortés, P., Parada, J. and Franco, W. 2016. Development of alginate microspheres containing thyme essential oil using ionic gelation. *Food Chemistry*, **204**: 77-83.

Cimanga, K., Tona, L., Apers, S., De Bruyne, T., Hermans, N., *et al.*, 2002. Correlation between chemical composition and antibacterial activity of essential oils of some aromatic medicinal plants growing in the Democratic Republic of Congo. *Journal of Ethnopharmacology*. **79**(2): 213-220.

CLSI. 2023. *Performance for Aantimicrobial Susceptibility Testing.* CLSI supplement M100 (33rd edn.). Clinical and Laboratory Standards Institute, USA. (*https://clsi.org/shop/standards/m100/*).

Das, S., Singh, V.K., Dwivedy, A.K., Chaudhari, A.K., Upadhyay, N., 2019. Encapsulation in chitosan-based nanomatrix as an efficient green technology to boost the antimicrobial, antioxidant, and *in situ* efficacy of *Coriandrum sativum* essential oil. *International Journal of Biological Macromol*ecules. **133**: 294-305.

Deepika, Chaudhari A.K., Singh, A., Das, S. and Dubey, N.K. 2021. Nanoencapsulated *Petroselinum crispum* essential oil: Characterization and practical efficacy against fungal and aflatoxin contamination of stored chia seeds. *Food Bioscience,* **42**: 1101117. (*https://doi.org/10.1016/j.fbio.2021.101117*].

Donsì, F., Annunziata, M., Sessa, M. and Ferrari, G. 2011. Nanoencapsulation of essential oils to enhance their antimicrobial activity in foods. *Journal of Food Science and Technol*ogy, **44**(9): 1908-1914.

Ghazali, M., Ismail, N., Zulkifli, M.F.R., Wan Nik, W.S., Umoren, S., *et al*. 2021. Employing *Cymbopogon citratus* (lemongrass) as an eco-friendly corrosion inhibitor for mild steel in seawater. *Journal of Sustainable Science and Management,* **16**(3): 71-82.

Hadidi, M., Pouramin, S., Adinepour, F., Haghani, S. and Jafari, S.M. 2020. Chitosan nanoparticles loaded with clove essential oil: Characterization, antioxidant, and antibacterial activities. *Carbohydrate Polymers,* **236**: 116075. [*https://doi.org/10.1016/j.carbpol.2020.116075*].

Hasani, M. and Hasani, S. 2018. Nano-encapsulation of thyme essential oil in chitosan-Arabic gum system: Evaluation of its antioxidant and antimicrobial properties. *International Journal of Biological Macromolecules,* **115**: 370-375.

Hassanshahian, M., Saadatfar, A. and Masoumipour, F. 2020. Formulation and characterization of nanoemulsion from *Alhagi maurorum* essential oil and study of its antimicrobial, antibiofilm, and plasmid curing activity against antibiotic-resistant pathogenic bacteria. *Journal of Environmental Health Science and Engineering,* **18**: 1093-1103.

Holley, R.A. and Patel, D. 2005. Improvement in shelf-life and safety of perishable foods by plant essential oils and smoke antimicrobials, *Food Microbiology*, **22**(4): 273-292.

Hosseini, S.F., Zandi, M., Rezaei, M. and Farahmandghavi, F. 2013. Two-step method for encapsulation of oregano essential oil in chitosan nanoparticles: Preparation, characterization, and *in vitro* release study. *Carbohydrate Polymers*, **95**(1): 50-56.

Jisha. 2020. *Effect of Lemongrass Oil and Citral in Combating Antibiotic Resistance in Staphylococcus aureus Isolates from Bovine Mastitis.* Ph.D. thesis submitted to the Kerala Veterinary and Animal Sciences University, Mannuthy, Thrissur, Kerala, India.

Kalemba D. and Kunicka A. 2003. Antibacterial and antifungal properties of essential oils. *Current Medicinal Chemistry,* **10**(10): 813-829.

Keawchaoon, L. and Yoksan, R. 2011. Preparation, characterization, and *in vitro* release study of carvacrol-loaded chitosan nanoparticles. *Colloids and Surfaces B: Biointerfaces,* **84**(1): 163-171.

Kotzekidou, P., Giannakidis, P. and Boulamatsis, A. 2008. Antimicrobial activity of some plant extracts and essential oils against foodborne pathogens *in vitro* and on the fate of inoculated pathogens in chocolate. *Food Science and Technology,* **41**(1): 119-127.

Kumar, N.M.R. 2000. Nano and microparticles as controlled drug delivery devices. *Journal of Pharmacy and Pharmaceutical Sciences.* **3**(2): 234-258.

Lertsutthiwong, P., Noomun, K., Jongaroonngamsang, N., Rojsitthisak, P. and Nimmannit, U. 2008. Preparation of alginate nanocapsules containing turmeric oil. *Carbohydrate Polymers,* **74**(2): 209-214.

Misra, R. and Sahoo, S.J. 2012. Antibacterial activity of doxycycline-loaded nanoparticles. *Methods in Enzymology*, **509:** 61-81.

Mukarram, M., Choudhary, S., Khan, M.A., Poltronieri, P., Khan, M.M.A., *et al*. 2021. Lemongrass essential oil components with potent antifungal properties. *Industrial Crops and Products.* **159:** 113045. [*https://doi.org/10.1016/j.indcrop.2020.113045*].

Mulani, M.S., Kamble, E.E., Kumkar, S.N., Tawre, M.S. and Pardesi, K.R. 2019. Emerging strategies to combat ESKAPE pathogens in the era of antimicrobial resistance: A review. *Frontiers in Microbiology,* **10**: [*https://doi.org/10.3389/fmicb.2019.00539*].

Naik, M.I., Fomda, B.A., Jaykumar, E. and Bhat, J.A. 2010. Antibacterial activity of lemongrass (*Cymbopogon citratus*) oil against some selected pathogenic bacteria. *Asian Pacific Journal of Tropical Medicine*, **3**(7): 535-538.

O'Neill, J. 2016. *Tackling Drug-Resistant Infections Globally: Final Report and Recommendations. Review on Antimicrobial Resistance*. Wellcome Trust and HM Government, UK. [*https://api.semanticscholar.org/CorpusID:36259397*].

Onawunmi, G.O. and Ogunlana, E.O. 1986. A study of the antibacterial activity of the essential oil of lemongrass (*Cymbopogon citratus*). *International Journal of Crude Drug Research*, **24**(2): 64-68.

Osundiya, O.O., Oladele, R.O. and Oduyebo, O.O. 2013. Multiple antibiotic resistance (MAR) indices of *Pseudomonas* and *Klebsiella* species isolates in Lagos University Teaching Hospital. *African Journal of Clinical and Experimental Microbiology.* **14**(3): 164-168.

Raut, J.S. and Karuppayil, S.M. 2014. A status review on the medicinal properties of essential oils. *Industrial Crops and Products*, **62**: 250-264.

Sanchez, E., Rivas Morales, C., Castillo, S., Leos-Rivas, C., Garcia-Becerra, L. and Ortiz Martínez, D.M. 2016. Antibacterial and antibiofilm activity of methanolic plant extracts against nosocomial microorganisms. *Evidence Based Complementary and Alternative Medicine*, **2016**: 1-8. [*https://doi.org/10.1155/2016/1572697*].

Schweiggert, U., Carle, R. and Schieber, A. 2007. Conventional and alternative processes for spice production - A review. *Trends in Food Science and Technology*. **18**(5): 260-268.

Shetta, A., Kegere, J. and Mamdouh, W. 2019. Comparative study of encapsulated peppermint and green tea essential oils in chitosan nanoparticles: Encapsulation, thermal stability, *in vitro* release, antioxidant, and antibacterial activities. *International Journal of Biological Macromolecules*, **126**: 731-742.

Sotelo-Boyás, M.E., Correa-Pacheco, Z.N., Bautista-Baños, S. and Corona-Rangel, M.L. 2017. Physicochemical characterization of chitosan nanoparticles and nanocapsules incorporated with lime essential oil and their antibacterial activity against food-borne pathogens. *Food Science and Technology,* **77:** 15-20.

Sykes, J.E. and Rankin, S.C. 2014. Isolation and identification of aerobic and anaerobic bacteria. pp. 17-28. **In:** *Canine and Feline Infectious Diseases* (ed. J.E. Sykes), Elsevier Inc., USA. [*https://doi.org/10.1016/B978-1-4377-0795-3.00003-2*].

EUCAST. 2020. 2020. *Clinical Breakpoints - Bacteria (v 10.0)*. The European Committee on Antimicrobial Susceptibility Testing. The EUCAST Website [*https://www.eucast.org/publications_and_documents/consultations/*].

Thomas, V.M., Brown, R.M., Ashcraft, D.S. and Pankey, G.A. 2019. Synergistic effect between nisin and polymyxin B against pandrug-resistant and extensively drug-resistant *Acinetobacter baumannii*. *International Journal of Antimicrobial Agents*, **53**(5): 663-668.

Veras, H.N.H., Rodrigues, F.F.G., Colares, A.V., Menezes, I.R.A., Coutinho, H.D.M., *et al.*, 2012. Synergistic antibiotic activity of volatile compounds from the essential oil of *Lippia sidoides* and thymol, *Fitoterapia*, **83**(3): 508-512.

WHO. 2014. *Antimicrobial Resistance: Global Report on Surveillance.* World Health Organization. Geneva, Switzerland.